MSc Sadegh Abbasnia[1,*]
MSc Vali Shafieyoun[2]
PhD student Mohammad Golzarijalal[3]
Dr Zarrin Nasri[1]

Computational fluid dynamics versus experiment: an investigation on liquid weeping of Nye tray

Abstract

In this study, the weeping phenomenon was investigated using some tests and a numerical model. The tests were performed within a 1.22 m-diameter pilot-scale column including two chimney trays and two Nye test trays by the air-water system. The rates of weeping were measured in Nye trays with two heights of the weir and a 5% hole area. Moreover, the weeping rate in outlet half and inlet half of the Nye tray and the total weeping rate were calculated. In the next step, an Eulerian-Eulerian CFD technique was used in the current study. The results show good agreement between the attained CFD findings and the experimental data.

Keywords: Weeping; CFD; Experiment; Nye tray

[1] Iranian Research Organization for Science and Technology (IROST), Department of Chemical Technology, Azadegan Highway, P.O. Box 33535111, Tehran, Iran

[2] Petroleum University of Technology, Ahwaz Faculty of Petroleum, Behbahani Highway, 7118361991, Ahwaz, Iran

[3] University of Melbourne, Department of Chemical Engineering, Parkville, Victoria 3010, Australia

* Corresponding author E-mail address: Sadeghabbasnia1981@gmail.com

1. Introduction

Combining empirical and related theoretical findings is essential for designing a distillation tray. An appropriate phase contact and an improvement in a tray's efficiency are achieved by a proper tray design. It has been proved that the trays possess suitable flexibility for operation in a satisfactory area of operation circumstances. This flexibility is called the tray's operation window or behavior diagram. This region is identified by the liquid and vapor rates. By a low vapor rate, tray efficiency declines by the liquid weeping; however, the force extends toward the above tray and the entrainment phenomenon takes place at a high vapor rate. Numerous distillation towers operate at a lower capacity compared to their design capacity. Hence, by determining the entrainment limits and liquid weeping of the trays, appropriate information can be obtained for enhancing the performance in

Please cite this article as doi: 10.1002/ceat.202000207

towers. The weep fraction and dry tray pressure drop are two main hydraulic factors determining the lower operation limit for a tray [1-3]. The sieve trays result in the leakage of liquid within the deck holes at low vapor rates and decrease its normal operation window. Furthermore, the weeping is regarded as a usual reason for the trays' mal-functions in chemicals, olefins, refineries, and gas plants [4]. Lockett et al. [5] computed the reduction of tray performance caused by weeping. They attempted to prolong the former analyses' applicability [6-8] for industrial towers by attending the point where the gas phase is not combined between the trays. Fasesan [9] calculated the liquid weeping rate in absorption trays by two equal trays. The focus of this study was on an absorption column with an air-water system. The results were gained by two independent approaches of dye trace and weep-age catch tray method. Additionally, this researcher utilized a chimney tray for measuring the rate of weeping for valve trays and sieve through a direct volumetric technique. The findings illustrated that liquid weeping is different between the trays. The obtained results indicated that by increasing the liquid load, the rate of weeping for a sieve tray working in the weeping trend increases linearly.

To utilize sieve tray towers for industrial uses more effectively, it is essential to have an enhanced theoretical understanding of the sieve tray hydraulics. In this regard, understanding some measurable and valuable parameters like pressure drop is essential but not enough. Hence, comprehending the detailed performances of instant liquid and vapor flows in the column is necessary. Previously, the mathematical models were developed to predict the liquid weeping and its rate [10-12] as alternative techniques to interpret a tray performance over weeping circumstances. A model was developed by Wijin [13] for lower operation limits of absorption and distillation trays. This author provided a novel technique to calculate the minimum gas flow rates of valve trays and sieve operating in the churn, bubble, and turbulent flow systems. Also, the researcher examined the association between tray efficiency and weeping. Mehta et al. [14] used the numerical method to investigate the hydrodynamic of perforated trays and presented detailed information in this regard. Furthermore, Yu et al. [15] and Liu et al. [16] assessed the hydrodynamic of the tray by two- dimensional model through CFD. They presented models focusing on the variations and ignored the liquid phase hydraulics along with the gas flow in the direction of the dispersion height. A transient three-dimensional CFD model was presented by Quarini and Fischer[17] to investigate the hydrodynamic of the perforated tray. In the mentioned model, the drag coefficient was constant and equal to 0.44. Moreover, the hydraulics of a sieve tray was enhanced by Krishna et al. [18] and Krishna and Van Baten[19] by approximating a novel drag coefficient for the large bubbles swarm in terms of the association of Bennett et al. [20] A three-dimensional model was presented by Gesit et al. [21] for predicting the flow patterns and hydraulics of the sieve tray by CFD device utilizing Colwell[22] association for the liquid holdup working well in the force direction. A three-dimensional CFD simulation was presented by Teleken et al. with the mathematical homogeneous biphasic model [23-25] for evaluating the effect of electrical resistance of heaters over the sieve tray surfaces and its hydrodynamics. Moreover, Teleken et al. assessed a falling liquid film's flow via a distillation column via an Eulerian-Eulerian CFD technique. They aimed to provide a better interpretation of the feed distribution system. Patwardhan and Yadav [26] and Ud Din et al. [27] presented CFD models for comprehending the sieve's hydrodynamics and pulsed-sieve plate extraction column using the Eulerian-Eulerian method and the standard k-ε turbulence model. Zarei et al. [28] studied the weeping phenomena in a circular sieve tray by experimental and CFD methods. The experiment was performed in a pilot-scale column with a diameter of 1.22 m including two chimney trays and two test trays. Some hydraulic parameters and weeping rates were calculated in sieve trays with a hole area of 7.04%. Overall, there was good consistency between the attained CFD findings and the experimental data. A 3D and biphasic model was presented by Yang et al. [29] for the tray without a downcomer (Ripple tray) using the CFD. The model was homogenous following Euler-Euler interaction. They compared some elements like the clear liquid's height in the tray with the sieve tray and reported that the Ripple tray without downcomer experiences a rather small pressure drop compared to the sieve tray. Moreover, its operational flexibility was enhanced in comparison to the sieve tray. In[30] the hydraulics and flow patterns of a valve tray were predicted utilizing computational fluid dynamics simulation and experimental method. A three-dimensional CFD model was presented in the Eulerian frame work. Experimental findings of the average liquid holdup, froth height, clear liquid height, dry pressure drop, and total pressure drop were investigated and compared with the CFD results. The CFD results were in good consistency with experimental results. CFD simulation and experimental study on bubble cap tray were done in [31]. Simulations were performed in industrial range of gas and liquid rates. Some hydrodynamic parameters were calculated and predicted. The gained results were in agreement with experimental results. Abbasnia et al. [32] investigated the efficiency and mass transfer for the Nye tray and sieve tray. The system in their investigation was methanol-normal propanol. The distributions of methanol compositions on the trays were obtained for four average methanol compositions. The results revealed that the liquid composition profile on the Nye tray is enhanced compared to the sieve tray and more resembling the rectangular tray. Nye tray's Murphree efficiency was almost 10% higher than the sieve tray. The present study aim to investigate the liquid weeping from the Nye tray using an experimental method and computational fluid dynamics (CFD). In the experimental method, a small column with a diameter of 1.22 m and four trays (two Nye trays and two chimney trays) were used. Since no experimental and CFD studies have been performed on liquid experimental from the Nye tray so far, the present study may be useful for further studies on this tray and similar trays. Also, considering the previous studies on liquid weeping from the sieve tray in similar dimensions, the results of this study can be compared to the studies about the sieve tray. Besides, in this study, a general comparison was made between liquid weeping from the Nye tray and sieve tray using the CFD method.

2. Experimental work

According to Fig. S1, the flowsheet design consists of a column with two chimney trays and two Nye trays. Three sight glasses are included in the column for facilitating the hydrodynamic phenomena observation over the trays. The air is blown by a blower through the column and water is pumped by a pump from a storing container inside the column to measure the water flow rate by a calibrated flow meter. Given the studied air/water system, the air outlet effluents to the surrounding. Inlet downcomer of the upper Nye tray is filled with rings. Table 1 represents the specifications of the trays. Besides, the gas velocity is measured utilizing a calibrated pitot tube located at the blower's exit and a chimney tray placed under the test tray gathers the liquid weeping from the test tray then it is brought back to the tank. The height of the separator baffle is crucial for determining the liquid wept from two halves of the tray. To prevent any effect on the gas distribution, the height of the separator baffle must be lower than the chimney caps, as well as it must prevent from overflowing between two sides [33, 34].

Table.1

Description	Industrial-scale tray	unit
Tower cross section diameter	1.22	m
Tray diameter	1.20	m
Hole diameter	0.0127	m
Weir length	0.925	m
Outlet weir heights	0.05, 0.075	m
Clearance under downcomer	0.025	m
% bubbling area (over total area)	76	%
% Hole area (over total area)	5	%
% Downcomer area	12.5	%
The height for the vertical part of The incoming panel for the Nye tray	0.05	m
Punched area under the Incoming downcomer	0.05	%
Tray thickness	0.0025	m

The comparison between the experimental data and numerical predictions was limited to the relatively restricted set of available computational power and experimental data in the literature. In this regard, the current experimental data can be useful for the readers concerning Nye trays.

3. CFD simulation

3.1. Framework

In the present research, two imperative multiphase models of Eulerian-Eulerian and volume of fluid (VOF) are utilized. The VOF method is a proper numerical technique to simulate the two-phase flows. The gas-liquid interface is a critical feature of this modeling. The model can be utilized to make the interface between the phases (a free surface reconstruction technique). This technique is also employed for mass and heat transfer in two-phase flows. In the present work, it was tried to assess the weeping rate of a column armed with Nye trays for the whole system not mainly for the gas-liquid interfaces. Consequently, an Eulerian-Eulerian method was chosen for this work. Here, two sets of transient CFD models in the 3D framework were established to investigate the single and two-phase flows via a full three-dimensional geometry of the circular distillation column. The Eulerian-Eulerian multiphase flow was utilized where the phases are treated as interpenetrating continua. Furthermore, the pressure velocity coupling was incorporated using the SIMPLE algorithm. To solve the transient equations before reaching the quasi mode, the time period of 0.002 s was considered. The upwind technique was also used for the advection discretization scheme and second-order backward Euler for integrating the time. The equations of momentum balance, species conservation, and mass conservation were solved but the energy conservation was neglected due to the isothermal system.

3.2. Basic equations

These two phases were modeled by transport equations. The transport equations (continuity, mass transfer, and momentum) were numerically solved for the two phases. The continuity equation is expressed as follows:

$$\frac{\partial(\varepsilon_L \rho_L)}{\partial t} + \nabla.(\varepsilon_L \rho_L u_L) = -S_{GL} \quad (1)$$

$$\frac{\partial(\varepsilon_G \rho_G)}{\partial t} + \nabla.(\varepsilon_G \rho_G u_G) = S_{GL} \quad (2)$$

Where S_{LG} shows the mass transfer rate from the liquid phase to the gas phase and vice versa. The local balance condition must be satisfied by the mass transfer between the phases, so $S_{LG} = -S_{GL}$.

The equation of momentum is as follows:

$$\frac{\partial(\rho_L \varepsilon_L u_L)}{\partial t} + \nabla.\left(\rho_L \varepsilon_L u\ _L u_L - \mu_L \varepsilon_L (\nabla u_L + (\nabla u_L)^T)\right) = -\varepsilon_L \nabla p - M_{G,L} + \rho_L \varepsilon_L g, \text{ and} \quad (3)$$

$$\frac{\partial(\rho_G \varepsilon_G u_G)}{\partial t} + \nabla.\left(\rho_G \varepsilon_G u_G u_G - \mu_G \varepsilon_G (\nabla u_G + (\nabla u_G)^T)\right) = -\varepsilon_G \nabla p + M_{G,L} + \rho_G \varepsilon_G g. \quad (4)$$

Here, ε_G and ε_L the volume fractions of the liquid and gas phases, respectively. Also,

$$\varepsilon_G + \varepsilon_L = 1. \quad (5)$$

The interphase momentum transfer (drag force), i.e., $\boldsymbol{M_{GL}}$, is evaluated as follows:

$$M_{GL} = \frac{3}{4} \rho_L \frac{\varepsilon_G}{d_G} C_D (u_G - u_L)|u_G - u_L|, \quad (6)$$

Where

C_D is the drag coefficient:

$$C_D = \frac{4}{3}\frac{\rho_L - \rho_G}{\rho_L} g d_G \frac{1}{{V_{Slip}}^2}, \quad (7)$$

V_{slip} is slip velocity:

$$V_{slip} = \frac{U_G}{{\varepsilon_G}^B}, \quad (8)$$

And ε_G^B and ε_L^B are the average volume fractions:

$$\varepsilon_L^B = exp\left[-12.55\left(U_G\sqrt{\frac{\rho_G}{\rho_L - \rho_G}}\right)^{0.91}\right], \text{ and} \quad (9)$$

$$\varepsilon_G^B = 1 - \varepsilon_L^B. \quad (10)$$

Finally, by replacing:

$$M_{GL} = \varepsilon_G(\rho_L - \rho_G) g \frac{\varepsilon_G^B}{U_G^2}(u_G - u_L)|u_G - u_L|, \quad (11)$$

Ultimately, the k−ε model was employed concerning the dispersed phase.

3.3. Boundary conditions and geometry

Taking into account two distinct drag coefficients for each section, the computational domain is divided into two parts. The upper section is initiated from the test tray deck to the outlet zone and the space under the test tray is the lower section where the liquid weeping appears under the special condition. The drag coefficient presented by Krishna et al. [18], which is independent of bubble diameter, is used in the upper space because of its extensive use by several researchers [18, 19, 30, 33]. Moreover, the heterogeneous and froth bubbly regimes are found in this domain for specific gas velocities. For the lower section, Grace's drag model is utilized, in which the liquid weeping is subjected to the upward gas stream[28].

$$C_D = \frac{4}{3}\frac{\rho_L - \rho_G}{\rho_L} g d_G \frac{1}{{U_T}^2}, \tag{12}$$

Fig. 1 represents the computational domain of the Nye tray. The Eulerian framework is utilized to investigate the weeping phenomena. Moreover, the utilized values of Fs for investigating the weeping phenomena are at the lower operation ranges. Based on the previous studies, a no-slip wall boundary condition is considered for the liquid phase, also, a free slip boundary condition is taken for the gas phase on the wall [15, 21, 32]. The liquid and gas phases are water and air at the atmospheric pressure and 25℃. Initially, the volume fractions of water and air for the tray are identified. The water volume fractions of 0.8 and 0.01 are adjusted for the dispersion height and the region above this height, respectively. Moreover, it is presumed that the downcomer is occupied with water to the height of 0.275. The superficial gas velocity is utilized as an initial guess for the gas velocity's vertical component throughout the computational domain. A uniform horizontal velocity distribution equivalent to the liquid inlet velocity is considered for the froth region as the other initial guess[28]. Also, a parabolic profile is taken for the liquid inlet velocity and the outlet and inlet liquid volume fractions are both presumed to be unity. It is of note that only the liquid is introduced to the downcomer clearance. Similarly, the gas phase goes to the vapor inlet and leaves the vapor outlet with the volume fractions of 1[28].

3.4. Mesh independency

In this section, the clear liquid height over the tray is determined for numerous meshes. The findings indicate that for the Nye tray, the optimal number of cells is 1,103,870. Table 2 illustrates the details of different meshes and Fig. S2 shows the meshing of the Nye tray.

Table 2

The clear liquid height (meter)	Number of cells
0.03667	673852
0.03578	961903
0.03483	**1103870**
0.03498	1275928
0.03485	1427395

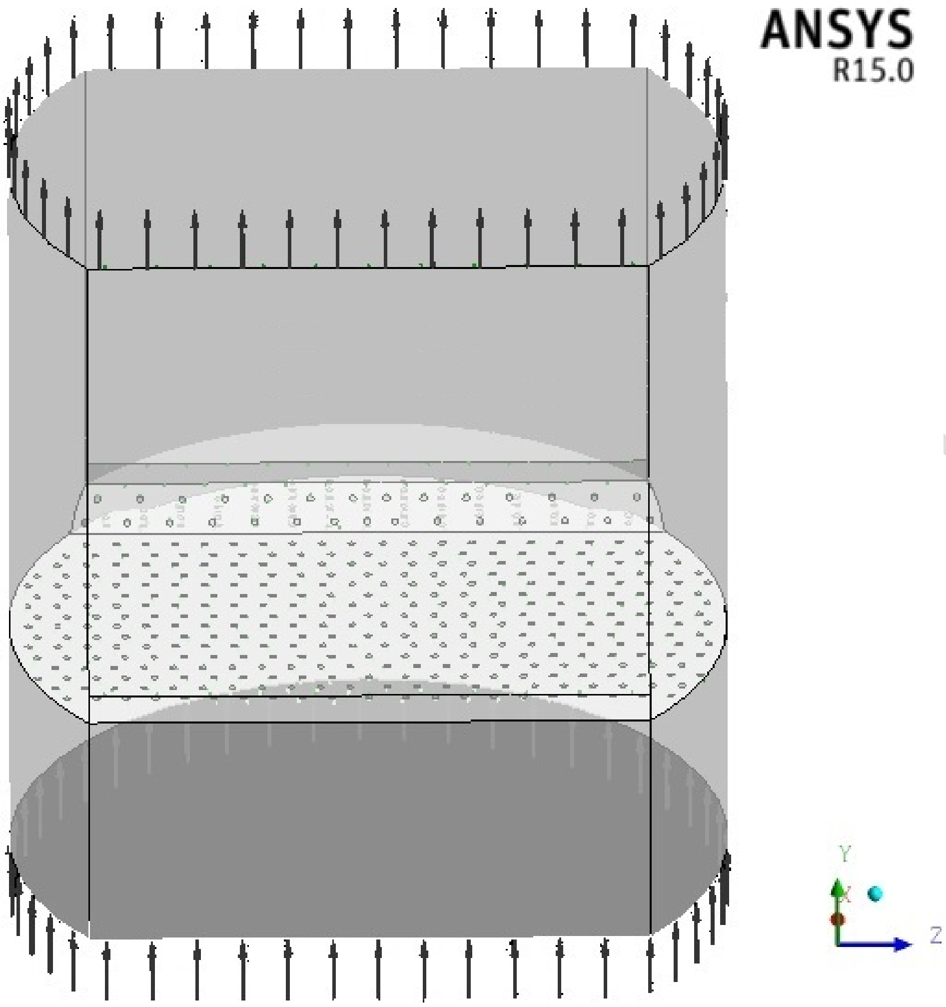

Figure.1

4. Results and discussion

4.1. CFD and experimental results

Over the tests, various values of Fs within the range of 0.27-1.21 m/s $(kg/m^3)^{0.5}$ and 3 liquid rates of 0.0053, 0.0105, and 0.0158 m^3/s were used. These operating circumstances are in the weeping range allowing better investigation of this occurrence. The liquid rate values were on the industrial scale as well. Moreover, two different heights of the weir are utilized in the test.

4.1.1. CFD and experimental results of dry pressure drop

Air was used as the gas phase for calculating the dry gas pressure drop, and the dry pressure drop for the tray was measured by blocking the inlet and outlet downcomer. The airflow was generated by the blower. After adjusting the airflow rate, it enters the chimney tray from the bottom of the column and it is distributed uniformly. A graduated manometer (its fluid is water) was used to measure the pressure difference between the two sides of the tray. The error of this manometer is about 5 Pa. One end of the manometer is placed about 5 cm below the tray and the other end of it is placed about 30 cm above the tray. In this research, the dry gas pressure drop test was performed in various F-factors of the air. The pressure difference between the two sides of the tray was obtained by changing the height of the liquid in the manometer tube. Fig. S3 shows the dry pressure drop of the Nye tray based on F_S.

The pressure drop of the gas flow in the single phase or dry state is one of the important parameters in designing the columns. This parameter indicates the amount of energy the gas loses when passing through the tray holes in the absence of liquid. To reduce this pressure drop, the area of the tray for passing the gas (perforated surface of the tray) should be increased. This is what was done in the Nye tray by adding the surface below the inlet downcomer to the perforated surface of the tray. In Fig. S3, the dry gas pressure drop increases with increasing gas factor (F_S), which is in agreement with experienced and experimental data. In the high gas flow rates, the results obtained by CFD show some deviation from the experimental values. This deviation is observed in most of CFD calculations. The reason for this deviation could be the chosen turbulence model for the system. Although the current models are suitable, they are still not quite accurate and cannot fully cover the complex behavior of the fluid.

4.1.2. CFD and experimental results at Q=0.0053 (m^3/s)

Figs. 2 and 3 show the liquid weeping rate for each tray half as a function of Fs respectively at $h_w = 5cm$ and $h_w = 7.5cm$ for Q=0.0053 (m^3/s) flow rate. As can be seen from these figures, weeping rates in the upstream are higher compared to the downstream for this flow rate. Fig. S4 confirms the results of Figs. 2 and 3. Based on these figures, higher heights of weir lead to the raising of liquid weeping from the tray deck.

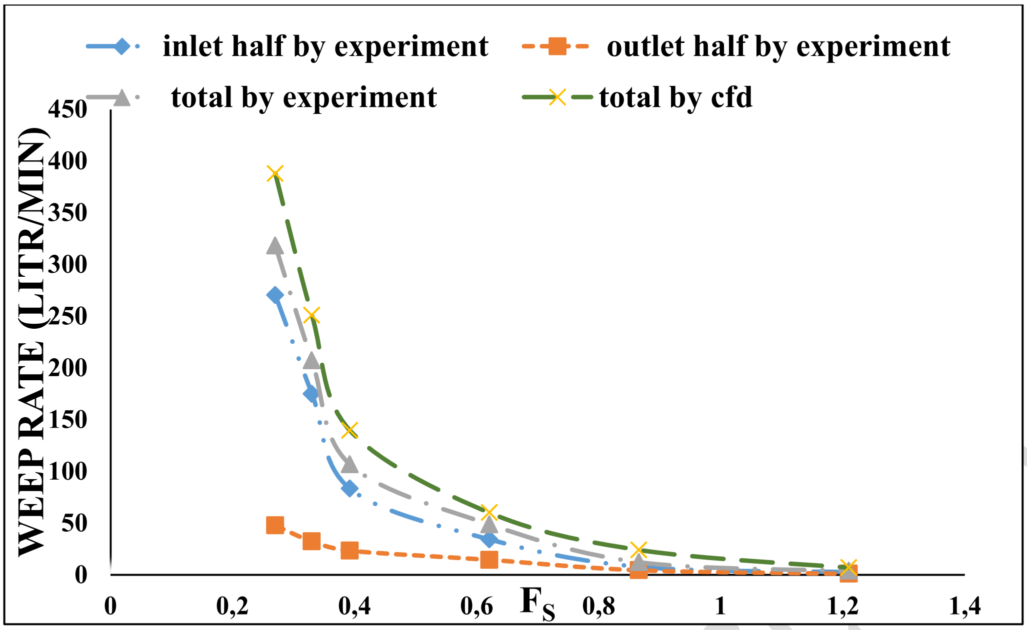

Figure.2

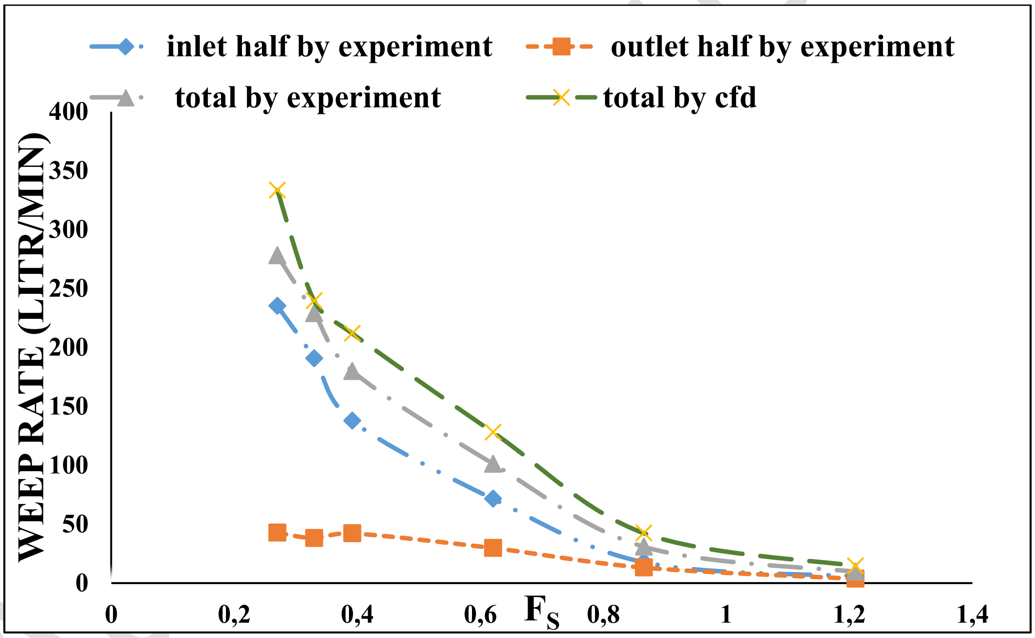

Figure.3

As can be seen from the curves, liquid weeping from the tray is strongly influenced by the gas factor (F_S). Also, it is seen that liquid weeping from the tray increases by decreasing the F_S. For this reason, the liquid weeping is considered as a limitation for gas flow. It seems that reducing the rate of the gas flow entering the column decrease the gas velocity in the tray holes and the dry pressure drop that keeps the liquid on the tray is reduced. This phenomenon causes liquid weeping from the tray holes and disturbs the uniform distribution of gas in the tray holes. In this case, the mean velocity of the gas passing through the tray holes is lower than the velocity in the dry state. As can be seen from the changing trend, the liquid weeping from the tray increases slightly with decreasing the F_S and then it increases extremely. Liquid weeping from the tray is somewhat tolerable, but by more growth, it will have severe adverse effects on the performance and efficiency of the column; so, it should be avoided as much as possible.

4.1.3. CFD and experimental results at Q=0.0105 (m^3/s)

Figs. 4 and 5 illustrate the liquid weeping rate for each tray half as a function of Fs respectively at h_w = 5cm and h_w = 7.5cm for Q=0.0105 (m^3/s) flow rate. For a low gas velocity range, the flow regime has a tendency toward the dumping or channeling weeping for both parts of the tray. Also, it is obvious that weeping rates in the downstream are more than those of the upstream for this flow rate and weir height is effective in the amount of tray weeping. Overall, increasing the weir height results in a subsequent increase in the clear-liquid height and an increase in the weeping rate (Figs. 4 and 5). Figs. 6 and 7 confirm these issues.

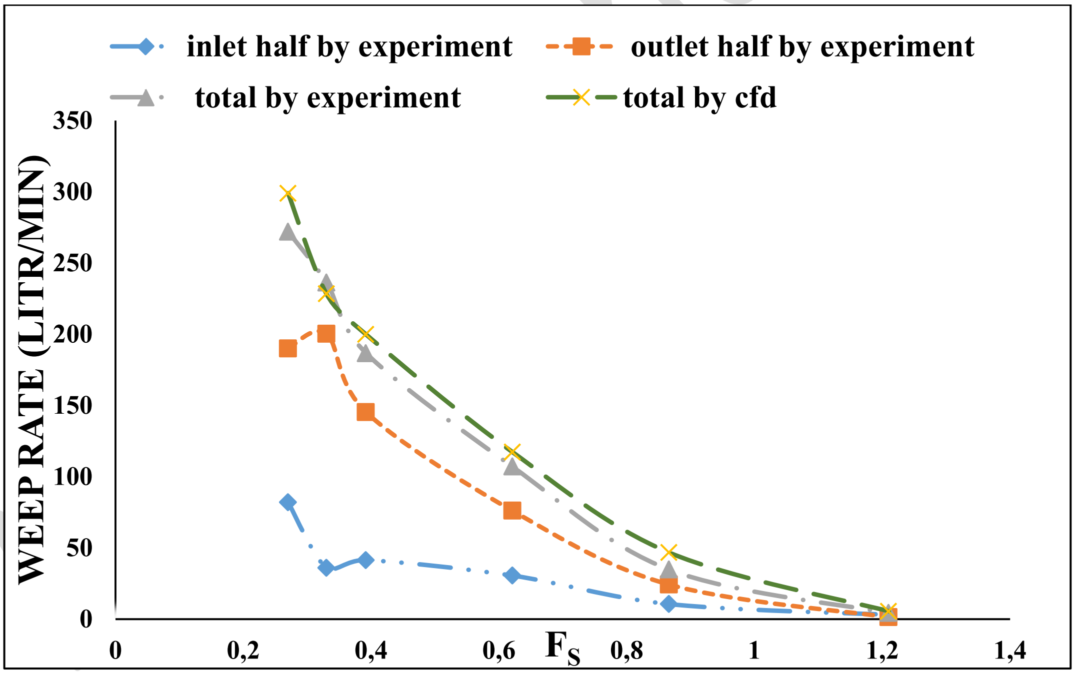

Figure.4

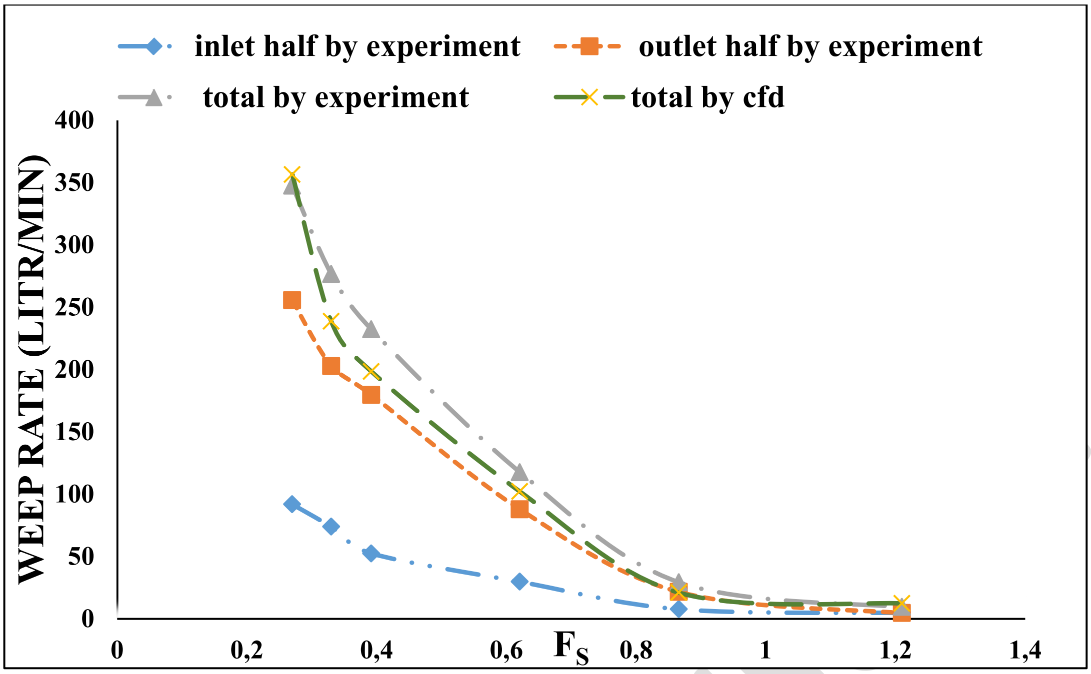

Figure.5

As expected, by decreasing F_S and increasing the rate of the liquid flow, the amount of liquid weeping increases. The increase is low at high F_S. As the rate of the gas flow decreases, the amount of liquid weeping increases with a higher rate. It seems that in F-factors close to the weeping point, the weeping mechanism is mainly drip and the weeping occurs randomly from some places and the liquid flow on the tray is far from the canalization. As the rate of the gas flow decreases further, some of the holes in the tray suddenly weep directly and continuously, and this is because of the imbalance of forces on the liquid of tray deck. In other words, by decreasing of gas flow rate, the force applied by the gas flow on the liquid decreases compared to the weight of the liquid, and the tray hole is simply involved in direct weeping instead of oscillating between bubbling and weeping. Direct weeping from the holes of the tray causes the canalization of the gas flow and canalization of the liquid flow on the tray. Thus, it is always necessary to avoid the mentioned state.

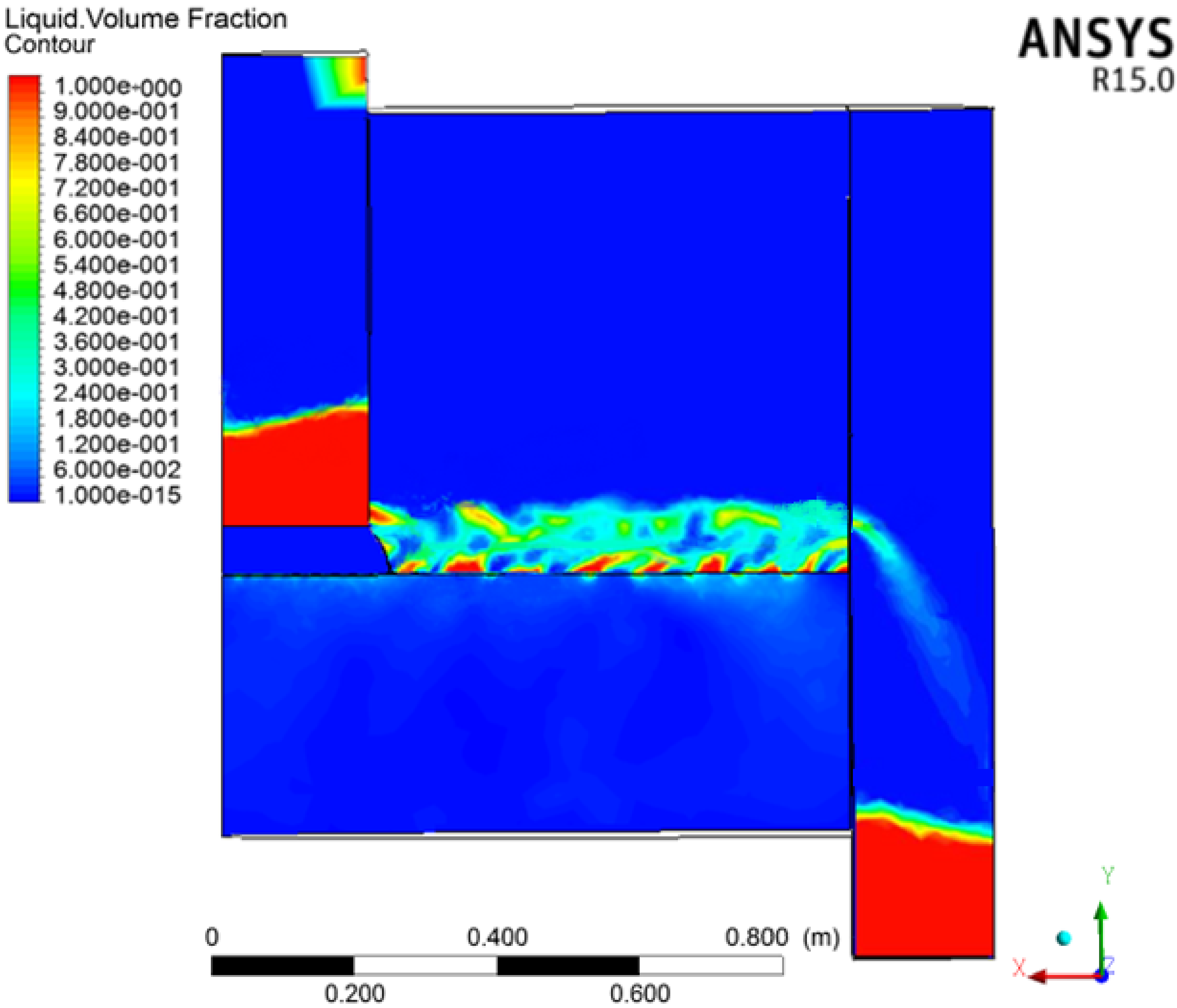
Liquid.Volume Fraction
Contour
1.000e-000
9.000e-001
8.400e-001
7.800e-001
7.200e-001
6.600e-001
6.000e-001
5.400e-001
4.800e-001
4.200e-001
3.600e-001
3.000e-001
2.400e-001
1.800e-001
1.200e-001
6.000e-002
1.000e-015
ANSYS
R15.0
0
0.400
0.800 (m)
0.200
0.600
Y
X
Z

Figure.6

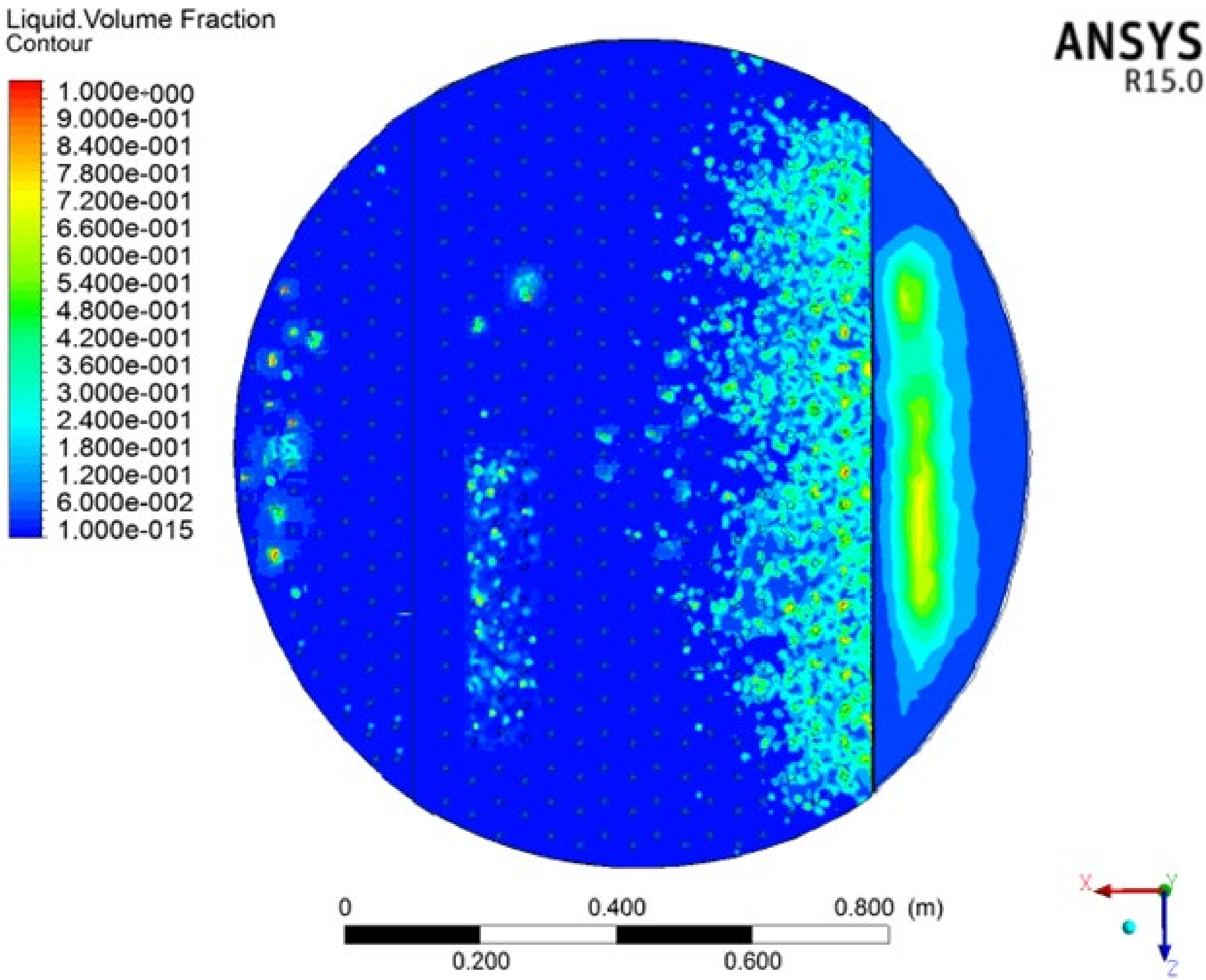

Figure.7

4.1.4. CFD and experimental results at Q=0.0158 (m^3/s)

Figs. 8 and 9 present the liquid weeping rate for each tray half as a function of Fs respectively at h_w = 5cm and h_w = 7.5cm for Q=0.0158 (m^3/s) flow rate. However, at high liquid rates, it is observed that changing the weir height from 5 to 7.5 cm has only a slight effect (Figs. 8 and 9). Weeping rates in the downstream are higher compared to the upstream for this flow rate. It is observed that different weeping rates in downstream and upstream of the tray decline with an increase in the gas flow rate. Figs. S5 verifies the results of Figs. 8 and 9.

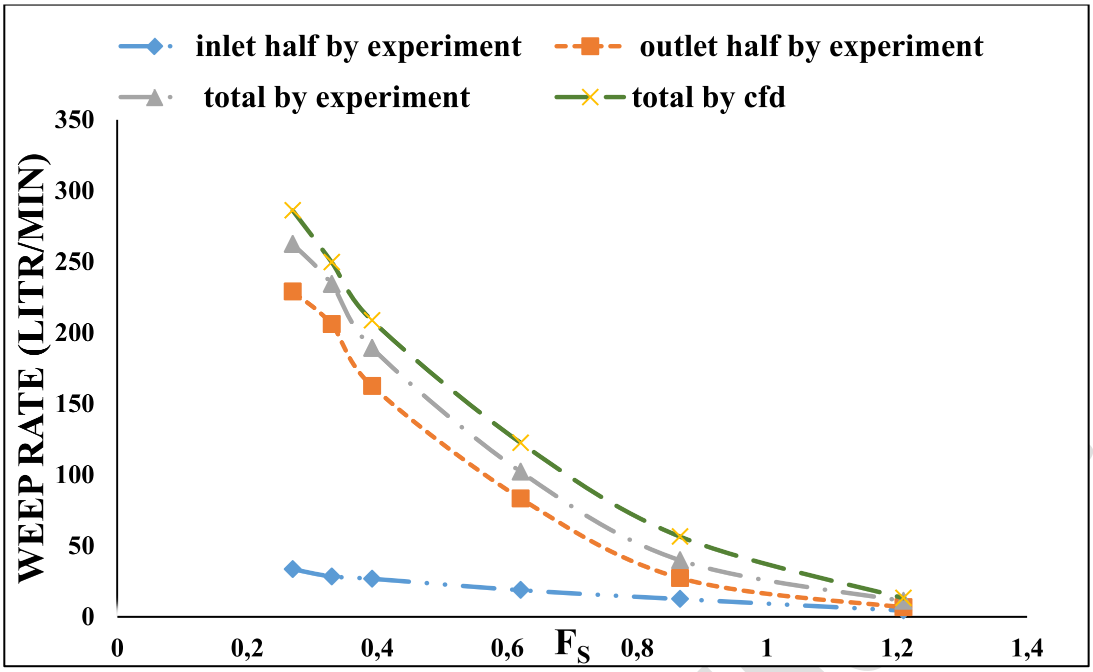

Figure.8

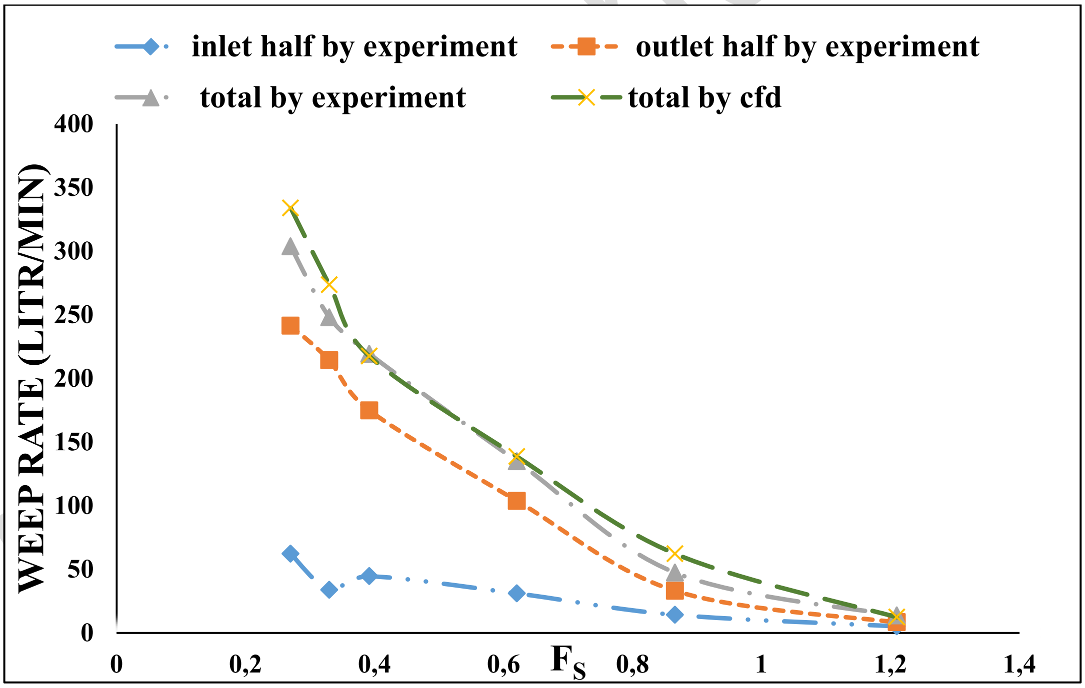

Figure.9

Under weeping conditions, some of the liquid passes through the outlet weir while the rest falls through the holes of tray. When the liquid is wept, it is not completely in contact with the passing gas, so the mass transfer in it occurs incompletely and reduces the efficiency of the tray. At the beginning and starting point of weeping, the efficiency decline is small, in the following, the rate of the gas flow decreases, this issue lead to more decrease of the efficiency. When the liquid weeping is large enough to reduce significantly the efficiency of the tray, the lower operating limit of the tray is reached. In this case, a part of the tray usually produces bubbles completely, while other parts of it may be completely weeping. It seems that in the Nye tray, with increasing liquid flow rate, the weeping phenomenon tends toward the second half of the tray. Thus, it would be concluded that in mentioned conditions, bubbling in the first half of the tray is more than it in the second half.

4.1.5. A limited CFD comparison between the Nye tray and the same sieve tray

Figs. S6 and 10 give the weep rates and liquid velocity vectors, respectively, for the Nye tray and the same sieve tray in Q=0.0105 (m^3/s), F_S=0.392 m/s (kg/m^3)$^{0.5}$, and $h_w = 5cm$. the difference between the weeping rate downstream and upstream for the Nye tray is more than it for the sieve tray . Furthermore, the total weeping rate for the Nye tray is close to the total weeping rate of the sieve tray but slightly higher. Fig. 10 shows that the velocity of water drops is almost uniform along with the Nye tray, where this parameter is ununiformed along with the sieve tray.

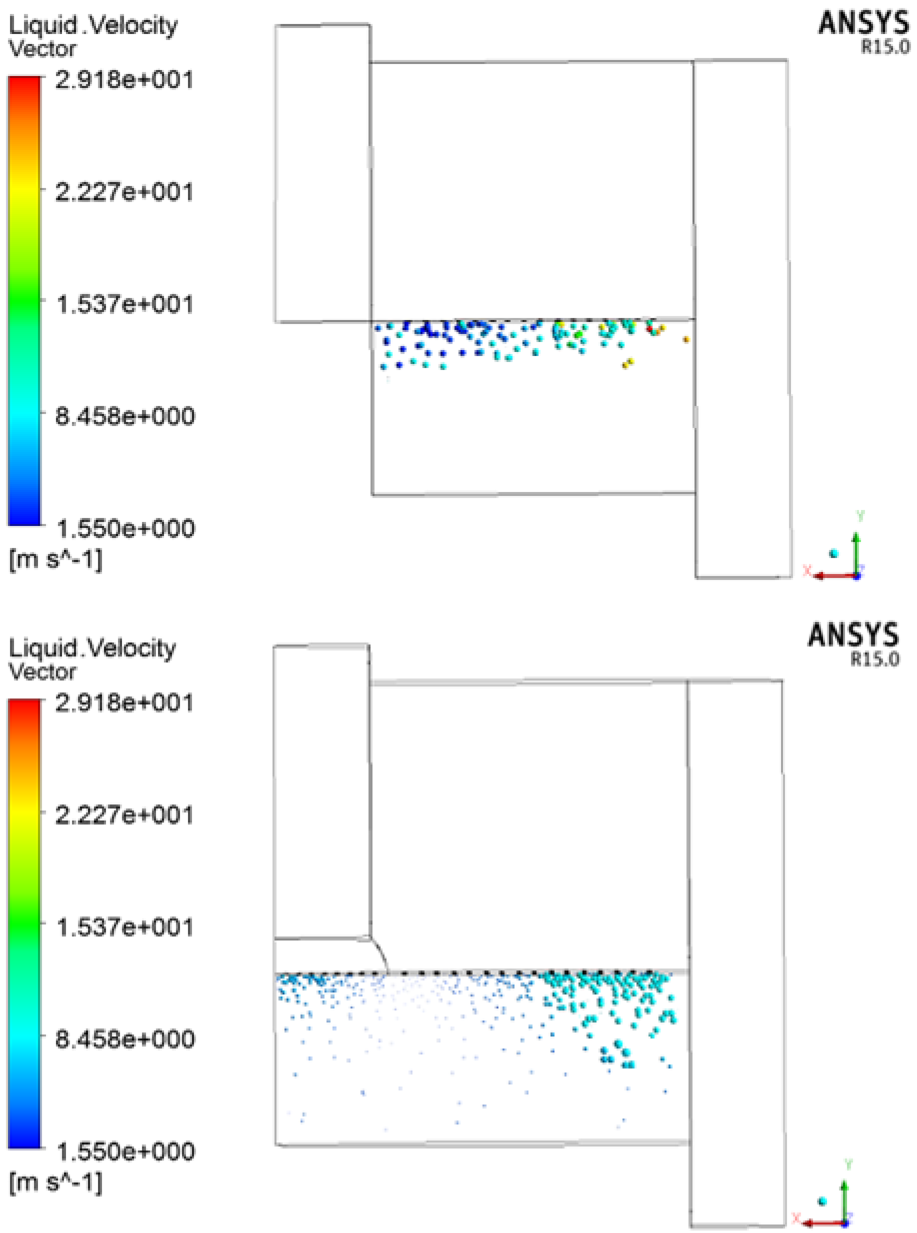

Figure.10

5. Conclusion

The liquid weeping as a key element in the performance of trays was investigated by the experiments and CFD model. A bunch of tests was carried out by the experimental tower in the industrial-scale where the experimental tower had two Nye trays and two chimney trays. The area of holes was 5% (based on total area).

The weeping in outlet and inlet sections of the tray and the total weeping rate were experimentally determined. It was found that the weeping rates in the inlet section of the Nye tray are higher compared to the outlet half of the Nye tray for low liquid flow rates where weeping rates were greater in outlet half of the Nye tray for middle and high liquid flow rates. Moreover, the difference between the weeping rate from downstream and upstream of the

Nye tray reduces by increasing the gas flow rate. Moreover, higher gas rates provide low weeping rates along with the tray, which may result in increased tray efficiency. Besides, it was observed that taller weir height increased weeping rate unless at high liquid rate. Through a limited comparison between Nye tray and the same sieve tray, it was revealed that weeping rates in the inlet of the sieve tray were higher compared to the outlet of the sieve tray. But concerning the Nye tray, weeping rates in the downstream were very larger rather than those in the upstream. It is noteworthy that some weep can be endured without noticeably affecting the tray efficiency. Some mass transfer from and to the weeping liquid happens to reduce the effect of bypassing on efficiency. Weeping from the exit section of the tray is not detrimental to tray efficiency to some extent compared to weeping from the inlet of the tray and is endured to a much higher level[3]. Regarding this issue, it is demonstrated that the Nye tray is suitable for operating in high liquid rates where weeping rates tend toward the outlet half of the Nye tray. Overall, it seems that the inlet panel of the Nye tray makes a higher capacity for tray where it leads to very low weeping rates from the inlet of the Nye tray. This specification is a positive point of Nye tray and may provide high efficiency compared to a sieve tray [35].

Symbols used

Greek letters

ρ	Density [kg m^{-3}]
ε	Volume fraction [-]
ε^B	Average volume fraction [-]
v	Velocity [m s^{-1}]
μ	Dynamic viscosity [Pa s]

Sub- and Superscripts

eff	Effective
G	Gas phase
g	Gas phase
i	part *i*
Lam	Laminar
l	Liquid phase
L	Liquid phase
n	n = 1, 2, 3, 4, …
Tur	Turbulent

Abbreviations

A_B	Bubble area of tray [m^2]
A_H	Total area of holes [m^2]
C_D	Drag coefficient [-]
$\boldsymbol{g}$	Gravitational acceleration [~ 9.8 m s^{-2}]
F_S	F-factor [m s^{-1} (kg m^{-3})$^{0.5}$]

h_c	Effective clear liquid height [m]
h_w	Height of weir [m]
L_w	Weir length [m]
$M_{G,\,L}$	Interphase momentum transfer [kg m^{-2}s^{-2}]
P	Pressure [Pa]
Q_{L}	Liquid volumetric flowrate [m^{3}s^{-1}]
R	Radius of the tray [m]
S_{GL}	Rate of mass transfer from gas phase to liquid phase [kg m^{-3}s^{-1}]
S_{LG}	Rate of mass transfer from liquid phase to gas phase [kg m^{-3}s^{-1}]
$U_{G,in}$	Hole gas velocity [m s^{-1}]
U_G	Gas phase superficial velocity based on the bubbling area [m s^{-1}]
U_T	Droplet terminal velocity [m s^{-1}]
V_G, u_G	Gas velocity [m s^{-1}]
V_L, u_L	Liquid velocity [m s^{-1}]
V_{Slip}	Slip velocity [m s^{-1}]
x	Coordinate position in the direction of liquid flow along tray [m]
x/L	Dimensionless coordinate position along tray [–]
y	Coordinate position in the direction of vapor flow across tray [m]
z/R	Dimensionless coordinate position across tray [–]
z	Coordinate position in the transverse direction to liquid flow across tray [m]

References

[1] M. W. Biddulph, *AIChE Journal*, **1975**, *21 (1),* 41-49. DOI: https://doi.org/10.1002/aic.690210104

[2] Summers, D. R. *AIChE Annu Meet, Austin, TX, Distillation Symposium*–Paper 228f 2004.

[3] H. Kister. Distillation design. 1992, New York: McGraw-Hill.

[4] H. Z. Kister, *Chem Eng Res Des*, **2003**, *81 (1),* 5-26. DOI: https://doi.org/10.1205/026387603321158159

[5] M. Lockett, M. Rahman, H. Dhulesia, *AIChE journal*, **1984**, *30 (3),* 423-431. DOI: https://doi.org/10.1002/aic.690300311

[6] Kageyama, O.*Tray efficiency of distillation tower with weeping.Kagaku Kogaku,* **1966**, *30,* 629.

[7] N. G. O'Brien, *Ind Eng Chem Process Des Dev*, **1966**, *5 (4),* 382-387. DOI: https://doi.org/10.1021/i260020a007

[8] Kageyama, O. *Chem. E. Symposium Series* **1969**.

[9] S. O. Fasesan, *Ind Eng Chem Process Des Dev*, **1985**, *24 (4),* 1073-1080. DOI: https://doi.org/10.1021/i200031a030

[10] W. Zhang, R. Tan, *Chem Eng Sci*, **2000**, *55 (24),* 6243-6250. DOI: https://doi.org/10.1016/S0009-2509(00)00215-3

[11] W. Zhang, R. Tan, *Chem Eng Sci*, **2003**, *58 (2),* 287-295. DOI: https://doi.org/10.1016/S0009-2509(02)00548-1

[12] W. Zhang, R. Tan, *Chem Eng Tech: Ind Chemi-Pla Equi-Process Eng-Biotech*, **2003**, *26 (11),* 1169-1175.DOI:https://doi.org/10.1002/ceat.200301822

[13] E. Wijn, *Chem Eng J*, **1998**, *70 (2),* 143-155. DOI: https://doi.org/10.1016/S0923-0467(98)00089-X

[14] B. Mehta, K. Chuang, K. Nandakumar, *Chem Eng Res Des*, **1998**, *76 (7),* 843-848. DOI: https://doi.org/10.1205/026387698525450

[15] K. T. Yu, X. Yuan, X. You, C. Liu, *Chem Eng Res Des*, **1999**, *77 (6),* 554-560. DOI: https://doi.org/10.1205/026387699526458

[16] C. Liu, X. Yuan, K. T. Yu, X. Zhu, *Chem Eng Sci*, **2000**, *55 (12),* 2287-2294. DOI: https://doi.org/10.1016/S0009-2509(99)00492-3

[17] Fischer, C. and G. Quarini *Three-dimensional heterogeneous modeling of distillation tray hydraulics*. AIChE annu meet 1998.

[18] R. Krishna, J. Van Baten, J. Ellenberger, A. Higler, R. Taylor, *Chem Eng Res Des*, **1999**, *77 (7),* 639-646. DOI: https://doi.org/10.1205/026387699526575

[19] J. Van Baten, R. Krishna, *Chem Eng J*, **2000**, *77 (3),* 143-151. DOI: https://doi.org/10.1016/S1385-8947(99)00164-3

[20] D. Bennett, R. Agrawal, P. Cook, *AIChE Journal*, **1983**, *29 (3),* 434-442. DOI: https://doi.org/10.1002/aic.690290313

[21] G. Gesit, K. Nandakumar, K. T. Chuang, *AIChE journal*, **2003**, *49 (4),* 910-924. DOI: https://doi.org/10.1002/aic.690490410

[22] C. J. Colwell, *Ind Eng Chem Process Des Dev*, **1981**, *20 (2),* 298-307. DOI: https://doi.org/10.1021/i200013a019

[23] J. Teleken, L. Werle, C. Marangoni, M. Quadri, R. Machado, *Bra j of petro and gas*, **2009**, *3 (3)*.

[24] J. G. Teleken, L. O. Werle, I. G. Parisotto, C. Marangoni, A. P. Meneguelo, A. Bolzan, R. A. Machado, in *Comput Aided Chem Eng*, Elsevier, **2012**, 845-849.

[25] J. G. Teleken, L. O. Werle, I. G. Parisotto, C. Marangoni, A. P. Meneguelo, R. A. Machado, in *Comput Aided Chem Eng*, Elsevier, **2010**, 73-78.

[26] R. L. Yadav, A. W. Patwardhan, *Chem Eng Res Des*, **2009**, *87 (1),* 25-35. DOI: https://doi.org/10.1016/j.cherd.2008.06.010

[27] G. U. Din, I. R. Chughtai, M. H. Inayat, I. H. Khan, N. K. Qazi, *Separ Purif Tech*, **2010**, *73 (2),* 302-309. DOI: https://doi.org/10.1016/j.seppur.2010.04.017

[28] A. Zarei, S. H. Hosseini, R. Rahimi, *Chem Eng Res Des*, **2013**, *91 (12),* 2333-2345. DOI: https://doi.org/10.1016/j.cherd.2013.03.006

[29] N. Yang, R. Zhang, B. Jiang, Z. Li, L. Zhang, Y. Sun, *J. Taiwan Inst .Chem. Eng*, **2015**, *53,* 6-14. DOI: https://doi.org/10.1016/j.jtice.2015.02.021

[30] T. Zarei, M. Farsiani, J. Khorshidi, *Korean J Chem Eng*, **2017**, *34 (1),* 150-159. DOI: https://doi.org/10.1007/s11814-016-0250-z

[31] F. K. Shenastaghi, S. Roshdi, N. Kasiri, M. H. Khanof, *Separ Purif Tech*, **2018**, *192,* 110-122. DOI: https://doi.org/10.1016/j.seppur.2017.09.055

[32] S. Abbasnia, Z. Nasri, M. Najafi, *Separ Purif Tech*, **2019**, *215,* 276-286. DOI: https://doi.org/10.1016/j.seppur.2019.01.010

[33] R. Krishna, J. Van Baten, *Chem Eng Res Des*, **2003**, *81 (1),* 27-38. DOI: https://doi.org/10.1205/026387603321158168

[34] M. Lockett, S. Banik, *Ind Eng Chem Process Des Dev*, **1986**, *25 (2),* 561-569. DOI: https://doi.org/10.1021/i200033a038

[35] S. Abbasnia, Z. Nasri, V. Shafieyoun, M. Golzarijalal, Can J Chem Eng , In Press.

Table and Figure captions

Table.1. Specifications of test Nye tray

Table.2. the clear liquid height unto the number of cells for Nye tray at F_S =0.462 m/s $(kg/m^3)^{0.5}$ And Q_L=0.00694(m^3/s)

Figure.S1. Schematic flow sheet

Figure.1. Geometric plan of Nye tray

Figure.S2. Meshing shape of the downcomer in entrance of the Nye tray and a part of tray deck

Figure.S3. dry pressure drop

Figure.2. Experimental and computational results of weep rates versus F_S at Q_L =0.0053 (m^3/s) and *hw*=5 (cm)

Figure.3. Experimental and computational results of weep rates versus Fs at Q_L =0.0053 (m^3/s) and *hw*=7.5 (cm)

Figure.S4. Liquid velocity vector at Q=0.0053 (m^3/s) and F_S=0.866 m/s $(kg/m^3)^{0.5}$ for h_W=5 (cm) and h_W=7.5 (cm)

Figure.4. Experimental and computational results of weep rates versus F_S at Q_L =0.0105 (m^3/s) and *hw*=5 (cm)

Figure.5. Experimental and computational results of weep rates versus F_S at Q_L =0.0105 (m^3/s) and *hw*=7.5 (cm)

Figure.6.The contour of liquid volume fraction at Q=0.0105 (m^3/s) and F_S=0.621 m/s $(kg/m^3)^{0.5}$ for h_W=5 (cm)

Figure.7.The contour of liquid volume fraction at Q=0.0105 (m^3/s) and F_S=0.621 m/s $(kg/m^3)^{0.5}$ for h_W=7.5 (cm)(a view from under the tray)

Figure.8. Experimental and computational results of weep rates versus F_S at Q_L =0.0158 (m^3/s) and *hw*=5 (cm)

Figure.9. Experimental and computational results of weep rates versus F_S at Q_L =0.0158 (m^3/s) and *hw*=7.5 (cm)

Figure.S5. Liquid velocity vector at Q=0.0158 (m^3/s) and F_S=0.332 m/s $(kg/m^3)^{0.5}$ for h_W=5 (cm) and h_W=7.5 (cm)

Figure.S6. Computational results of weep rates for both trays (sieve and Nye) at Q=0.0105 (m^3/s) and F_S=0.392 m/s $(kg/m^3)^{0.5}$ and h_W=5 (cm)

Figure.10. Liquid velocity vector at Q=0.0105 (m^3/s) and F_S=0.392 m/s $(kg/m^3)^{0.5}$ and h_W=5 (cm) for the Nye tray and the same sieve tray

Supporting Information are available